

NASA Technical Memorandum 100885

## Bithermal Fatigue of a Nickel-Base Superalloy Single Crystal

(NASA-TM-100885) BITHERMAL FATIGUE OF A  
NICKEL-BASE SUPERALLOY SINGLE CRYSTAL  
(NASA) 15 p CSCL 11F

N88-22168

Unclas  
G3/26 0142337

Michael J. Verrilli  
*Lewis Research Center*  
*Cleveland, Ohio*

May 1988

**NASA**

# BITHERMAL FATIGUE OF A NICKEL-BASE SUPERALLOY SINGLE CRYSTAL

Michael J. Verrilli  
National Aeronautics and Space Administration  
Lewis Research Center  
Cleveland, Ohio 44135

## SUMMARY

The thermomechanical fatigue behavior of a nickel-base superalloy single crystal was investigated using a bithermal test technique. The bithermal fatigue test was used as a simple alternative to the more complex thermomechanical fatigue test. Both in-phase and out-of-phase bithermal tests were performed on  $\langle 001 \rangle$ -oriented coated and bare René N4 single crystals. In out-of-phase bithermal tests, the tensile and compressive halves of the cycle were applied isothermally at 760 and 982 °C respectively, while for the in-phase bithermal tests the temperature-loading sequence was reversed. The bithermal fatigue lives of bare specimens were shorter than the isothermal fatigue lives at either temperature extreme when compared on an inelastic strain basis. Both in-phase and out-of-phase bithermal fatigue life curves converged in the large strain regime and diverged in the small strain regime, out-of-phase resulting in the shortest lives. The coating had no effect on life for specimens cycled in-phase; however, the coating was detrimental for isothermal fatigue at 760 °C and for out-of-phase fatigue under large strains.

## INTRODUCTION

Current life prediction and constitutive models for elevated temperature service applications are usually based on isothermal fatigue data. In reality, components which see high temperature experience combinations of thermal and mechanical strains, or thermomechanical loading. For many alloys, thermomechanical fatigue (TMF) lives have been found to be significantly lower than those for fatigue at the minimum or maximum cycle temperatures (refs. 1 and 2). This problem is of particular concern in the gas turbine engine industry. Hot section components such as turbine blades and vanes not only experience severe thermomechanical strain cycling during engine service, but are also susceptible to oxidation and hot corrosion due to the high cycle temperatures. For use as turbine blades, nickel-base superalloy single crystals have been shown to have significantly improved creep rupture lives and elevated temperature fatigue strength than their conventionally cast counterparts. In addition, protective coating systems applied to superalloys markedly improve their oxidation and hot corrosion resistance. There is concern, however, that these coatings may degrade the mechanical properties of coated hardware.

The purpose of this work is to study the thermomechanical fatigue behavior of a coated single crystal, René N4, and, in particular, to study the effect of the coating on fatigue life. The coating system studied is an aluminide coating, Codep B-1. A bithermal test technique has been used as an alternative to the more conventional thermomechanical fatigue cycle.

## MATERIALS AND TEST PROCEDURES

René N4 was developed by the General Electric Company specifically for application as cast single crystal blades for aircraft gas turbine engines. The composition of this alloy, in weight percent, is: 9.25 Cr, 7.7 Co, 1.5 Mo, 6.0 W, 4.0 Ta, 0.5 Cb, 3.7 Al, 4.2 Ti, balance Ni. The heat treatment consists of a solution anneal at 1265 °C for 2 hr, followed by aging at 1080 °C for 4 hr, and finally 900 °C for 16 hr. The heat treatment was performed in a protective atmosphere. Typical as heat treated microstructure of René N4 is shown in figure 1. The alloy has a  $\gamma$ - $\gamma'$  structure, the  $\gamma'$  occupying about 65 percent by volume. The  $\gamma'$  particles are generally cuboidal, having an average edge width of  $0.030 \pm 0.010$   $\mu\text{m}$ . Some of the  $\gamma'$  is present in interdendritic eutectic pools and occupy about 0.4 percent by volume. The single crystals exhibited significant porosity, about 0.4 vol %.

Low cycle fatigue (LCF) specimens were machined from cast slabs such that the specimen axis was within 10° of the  $\langle 001 \rangle$  direction. Orientations were verified by x-ray diffraction. The low cycle fatigue specimens are shown diagrammatically in figure 2. The two slightly different geometries were the result of a misunderstanding.

The coating system studied was a diffusion aluminide coating developed by General Electric, Codep B-1 (ref. 3). The coating was applied by the pack cementation process to the machined specimens. The coated specimens received the same heat treatment as the bare specimens. The microstructure of the coating is shown in figure 3. The coating produced by the Codep B-1 process consists of an additive layer of NiAl with some embedded alpha  $\text{Al}_2\text{O}_3$  particles, and a fingered diffusion zone (ref. 3). The fingers are a sigma phase, with MC carbides and NiAl often present (ref. 3). The alloy structure of the coated specimens is the same as that observed for the bare specimens, since the heat treatment cycles are identical. Coating thickness as measured using optical microscopy was found to be about 0.055 mm, however the actual measured increase of specimen diameter was about 0.020 mm, indicating that some of the coating is formed by diffusion into the substrate material.

Fatigue tests were performed using a 90 kN closed loop, servo-hydraulic test system. A high temperature axial extensometer was employed for strain measurement. Specimens were heated by a radio frequency induction generator, taking care to minimize temperature variations along the gauge length to at most  $\pm 5$  °C. Temperature was measured using a chromel-alumel thermocouple. The ends of the thermocouple were rolled flat, then slightly overlapped and welded together. The thermocouple was looped around the specimen and spring loaded to hold the junction in contact with the gauge length. A disappearing wire pyrometer was used to verify the accuracy of the thermocouple readings. Temperature was controlled by a closed loop general purpose controller.

Isothermal LCF tests were performed at the upper and lower temperatures of the TMF cycle, namely 982 and 760 °C. The specimens were cycled in axial strain control at a frequency of 0.1 Hz. A digital waveform generator was used to produce a sinusoidal control waveform, with an R ratio of -1 (R = minimum strain/maximum strain). Both coated and bare specimens were tested at the two temperatures.

A bithermal test technique was employed to perform the TMF tests. This technique has been recently proposed as a simplified alternative to the more conventional TMF test (ref. 4). A schematic of an out-of-phase bithermal cycle is shown in figure 4. Mechanical loads are applied at the two temperature extremes of the cycle. The temperature excursions occur while the specimen is held at zero load. As illustrated in figure 4(a), the tensile and compressive strains are imposed at the low and high temperature, respectively, for the out-of-phase bithermal cycle. For an in-phase cycle, the loading sequence is reversed, i.e., the tensile loads are imposed at the high temperature and the compressive loads at the low temperature (fig. 4(b)). A 16-bit computer was used to generate the temperature and load waveforms which compose the bithermal cycle. Both coated and uncoated specimens were tested in out-of-phase and in-phase bithermal fatigue.

A control problem was encountered during the first five to ten cycles of all tests which necessitated slight modification of the test procedure. At 760 °C René N4 exhibits flat yielding behavior beyond the yield point of its stress-strain response (ref. 5). Deformation beyond the yield point was found to occur very rapidly regardless of the applied strain rate. This phenomena occurred during the first five to ten fatigue cycles and during this period the test system under computer control could not respond quickly enough to reverse the loading at the desired strain limit. Therefore, the first ten cycles of the tests were performed manually in stroke control using the setpoint control of the servocontroller to cycle between the two strain limits. The rest of the testing was performed using the computer in the load control mode.

## RESULTS

### Fatigue Lives

The isothermal and bithermal fatigue data are given in table I. The isothermal and bithermal fatigue lives are plotted in a total mechanical strain basis in figure 5. The lines shown are least square fits to the bare specimen data.

Both the coated and uncoated specimens had longer lives at 760 °C than at 982 °C. The coated specimen fatigued at 760 °C with a strain range of 1.6 percent had a life about one order of magnitude lower than an uncoated specimen with approximately the same strain range. Since only one coated specimen was tested at 982 °C the effect of the coating on life could not be determined conclusively.

In-phase bithermal fatigue lives seemed to be unaffected by the presence of the coating. Similar cyclic lives were observed for the coated and bare specimens over the strain ranges tested. However, out-of-phase bithermal test results showed life differences for the coated and bare specimens. In the low strain regime the coated and bare specimens produced similar lives. In the large strain regime, however, the coated specimens had much shorter lives than the bare specimens.

Comparing the bithermal to the isothermal lives one can see that specimens fatigued at 760 °C had the longest lives. In the low strain regime in-phase bithermal lives were greater than out-of-phase. However, in the high strain

regime out-of-phase bithermal fatigue resulted in longer lives than in-phase bithermal fatigue. With the exception of the high strain regime the out-of-phase bithermal lives are about the same as isothermal fatigue lives at 982 °C.

Fatigue lives can also be examined on an inelastic strain basis. The inelastic strain-life plots for the bare specimens are presented in figure 6. The lines plotted for the isothermal data are the least squares fit and trend curves are drawn for the bithermal data. The inelastic strains measured at half life are plotted. Isothermal fatigue resulted in longer lives than bithermal cycling. In the large strain short life regime, the two bithermal life lines appear to converge, however, in the small strain long life regime in-phase cycling resulted in significantly longer lives than out-of-phase cycling. Isothermal fatigue at 760 °C resulted in lower lives than fatigue at 982 °C as one might expect since the ductility of René N4 is lower at 760 °C than 982 °C (ref. 5).

### Fractography

All of the specimens were examined by optical microscopy and scanning electron microscopy after failure. In bare specimens fatigued at 760 °C cracks were found to initiate at surface and near surface microporosity. Initially, cracking occurred in a stage II manner and transitioned to a stage I mode on (111) planes, just as reported by Gabb et al. (ref. 6). Stage II crack growth dominated in fatigue tests at large strains. Figure 7 shows a fractograph of a coated specimen fatigued at 760 °C. Cracks initiated at the coating surface. Crack growth near the surface was in a stage II manner.

For bare specimens fatigued at 982 °C crack initiation occurred at surface micropores and oxide cracks (ref. 6). These oxide cracks were typically normal to the stress axis and were very abundant. Only stage II cracking was observed at this temperature. Crack initiation occurred at internal pores in the coated specimen fatigued at 982 °C (fig. 7). Once again only stage II cracking was observed.

Figure 8 shows a comparison of the fracture surface of coated and bare René N4 fatigued under in-phase bithermal cycling. In both the coated and bare specimens crack initiation occurred at large internal pores ( $>100\text{ }\mu\text{m}$ ). During long-term tests on bare specimens the spallation of the oxide was observed. Although surface cracks were found in sections of failed coated specimens none of these cracks penetrated the superalloy substrate.

Crack initiation of bare specimens in out-of-phase tests occurred at the surface as shown in figure 9. In tests at large strains, crack initiation occurred at surface porosity, however little model II fatigue crack growth was found around the initiation site. Final failure occurred along (111) planes as was the case in isothermal tests at 760 °C. The initiation at small strains also occurred at the surface but did not appear to be associated with porosity.

For the out-of-phase tests on coated specimens at strains greater than about 1.3 percent crack initiation occurred at the surface. It was quite obvious that these were associated with the coating. Many large circumferential cracks were found on the failed crystals (fig. 9(b)). For coated specimens fatigued at strains less than about 1.3 percent crack initiation was the same

as that observed for the uncoated specimens fatigued under the same strains, namely surface annular cracks. These surface annular cracks were not the result of brittle failure of the coating.

## DISCUSSION

### TMF Versus Bithermal

The pros and cons of the bithermal test as a method to study the combined effect of cyclic thermal and mechanical strains are discussed by Halford (ref. 4). For purposes of discussion it is instructive to briefly list some of the advantages and disadvantages of the bithermal test relative to a continuously-varying-temperature thermomechanical fatigue test. Bithermal fatigue introduces high- and low-temperature deformation within the same cycle but one can limit the number of active mechanisms by proper choice of temperatures, stress levels and hold times. The bithermal test captures the effect of thermal free expansion mismatch straining between the substrate and an oxide or coating. Other advantages of the bithermal technique are (1) there is little difficulty in synchronizing the temperature and strain waveforms and (2) the thermal free expansion strains are easily subtracted from the total (thermal plus mechanical) strains. Bithermal fatigue can lead to misleading results if simultaneously applied mechanical and differential expansion strains are important to life. Holding the specimen at zero load during the temperature excursions can allow undesirable recovery processes to occur. Since all of the thermal strains occur at the two temperature extremes during a bithermal cycle, any thermal free expansion differences would be more severe than those occurring during a thermomechanical fatigue cycle in which the temperature is continuously varying.

### Isothermal Versus Bithermal

A plot of the isothermal and bithermal fatigue lives on a total strain basis (fig. 5) is typically used to compare isothermal lives with nonisothermal lives because of difficulties in accurately determining the inelastic strain of a continuously-varying-temperature thermomechanical hysteresis loop. A comparison of the inelastic strain - life (fig. 6) may be more instructive in trying to understand the effect of the different types of cycling on fatigue life.

On an inelastic strain basis, bithermal fatigue is more damaging to the bare René N4 than isothermal fatigue at either the high temperature or the low temperature of the cycle. Gayda et al. (ref. 7) studied the bithermal fatigue of another superalloy single crystal, PWA 1480, coated with an overlay coating. This alloy is very similar to the René N4 alloy used in this study. Their data for both coated and bare specimens is plotted with the bare René N4 data on an inelastic strain basis in figure 10. Curves shown are trend curves. Gayda saw no differences between bare and coated life data for the alloy and coating which he studied. Although temperature extremes of the bithermal cycles are different in the two studies, results of the PWA 1480 alloy group closely with the René N4 data. Gayda found that for both in-phase and out-of-phase bithermal fatigue life in the large inelastic strain regime was limited by the ductility of the superalloy at the low temperature. In addition they suggested that for small inelastic strains crack initiation occurred much more easily

during out-of-phase bithermal fatigue than during isothermal fatigue at either the high or low temperature of the bithermal cycle. The coincidence of the two sets of data in figure 10 tends to suggest that these mechanisms could be operating during the bithermal fatigue of René N4. Not enough data were generated on the coated specimens to draw any conclusions.

### Effect of Coating

For isothermal fatigue at 760 °C life was shorter for the coated specimens than for the bare specimens. Crack initiation sites shifted from internal porosity for the bare specimens to the surface of coated specimens. Aluminide coatings of this type are generally brittle in this temperature regime (ref. 8) and therefore crack initiation in the coating can occur quite easily as it has a low fracture strain under these conditions.

Although only one coated specimen was fatigued at 982 °C the shift of crack initiation from surface micropores and oxide cracks for bare specimens to internal micropores for the coated specimen suggests that the oxidation protection of the coating effectively prevented surface initiation. This might increase the fatigue life of the coated crystals over the uncoated crystals at the high temperature. Additional fatigue testing would be necessary to determine the effect of the coating on fatigue life of René N4 at 982 °C.

For in-phase cycles, fatigue lives and crack initiation sites were the same for both the coated and bare specimens. Therefore it does not appear as if the coating had any affect on fatigue life for the in-phase case. Strangman and Hopkins (ref. 9) postulated that for in-phase thermal fatigue of coated superalloys the coating would experience relatively large compressive strains at the low temperature and relatively small tensile strains at the high temperature as a result of thermal expansion differences between the substrate and coating, and geometrical constraints imposed on the coating by the substrate. Addition of the mechanical strains imposed during the in-phase bithermal cycle would result in a small compressive strain or perhaps even a small tensile strain in the coating at the low temperature, depending, of course, on the magnitude of the imposed mechanical strain. At the high temperature of the in-phase bithermal cycle tensile strains will dominate in the coating. The combination of thermal mismatch strains and mechanical strains during in-phase cycling will result in strains in the coating which are generally much less than the fracture strain of the coating at both temperatures. Therefore in the life regime where cracks initiate at internal porosity during in-phase bithermal fatigue one would not expect the coating to effect life significantly.

Strangman and Hopkins' analysis (ref. 9) of out-of-phase thermal fatigue of coated superalloys predicts that significant tensile strains would develop in the coating at the low temperature due to thermal fatigue alone. The addition of tensile mechanical strains at the low temperature may result in strains greater than the fracture strain of the coating. The large reduction in life for coated René N4 at high strains as compared to the bare specimens is probably due to this phenomena.

## In-Phase Versus Out-of-Phase

In-phase bithermal cycling of both the coated and bare single crystals resulted in crack initiation at subsurface micropores, while out-of-phase cycling was characterized by surface crack initiation. With the exception of large strain, out-of-phase tests on coated specimens, in-phase and out-of-phase lives appear to converge at large strains and diverge in the small strain regime, with out-of-phase lives being the shortest. One possible reason for longer in-phase lives in the small strain regime may be the differences in crack initiation lives. Surface cracks were observed on bare specimens cycled out-of-phase or in-phase. However, the oxide tended to spall off during in-phase cycling, effectively blunting the surface cracks that formed in the oxide scale. Cracks initiated in the oxide scale during out-of-phase cycling were not blunted by oxide spallation and therefore could advance into the substrate and continue to grow. The compressive stresses that caused oxide spallation during in-phase bithermal cycling of bare specimens probably aided in blunting surface cracks in coated specimens. The tensile stresses developed during out-of-phase cycling probably lead to surface initiated failures in the coated specimens. For fatigue under large strains environmental attack became less important and the ductility of the alloy dictated the fatigue life.

### SUMMARY

1. The low cycle thermomechanical fatigue behavior of a nickel-base superalloy single crystal, René N4, both with and without a diffusion-aluminide coating, was studied using a bithermal test technique.
2. In the temperature regime of 760 to 982 °C, the bithermal fatigue lives of bare specimens were shorter than the isothermal fatigue lives at either temperature extreme when compared on an inelastic strain basis. Both in-phase and out-of-phase bithermal fatigue life curves converged in the large strain regime and diverged in the small strain regime, out-of-phase bithermal fatigue resulting in the shortest lives.
3. Isothermal fatigue of bare specimens resulted in a different initiation mode at the two temperatures. For bare specimens, surface oxide spike initiation occurred at 982 °C and surface porosity was the initiation site at 760 °C. For coated specimens, the initiation site shifted to internal pores at 982 °C and to mechanical cracking of the coating at 760 °C. The coated specimens had significantly shorter lives than bare specimens at 760 °C.
5. Out-of-phase bithermal fatigue also resulted in several crack initiation modes. For small strains initiation was the same as was observed for fatigue at 982 °C. For large strains, bare specimens cracked in the same manner as in fatigue of bare specimens at 760 °C, and coated specimens failed in the same fashion as coated specimens at 760 °C. In the large strain regime, the coated specimens had much shorter lives than bare specimens. In the small strain regime lives were the same for the coated and bare specimens.
6. The coating had no effect on life of specimens cycled in-phase for the strain regimes tested. In all cases crack initiation occurred at internal pores.



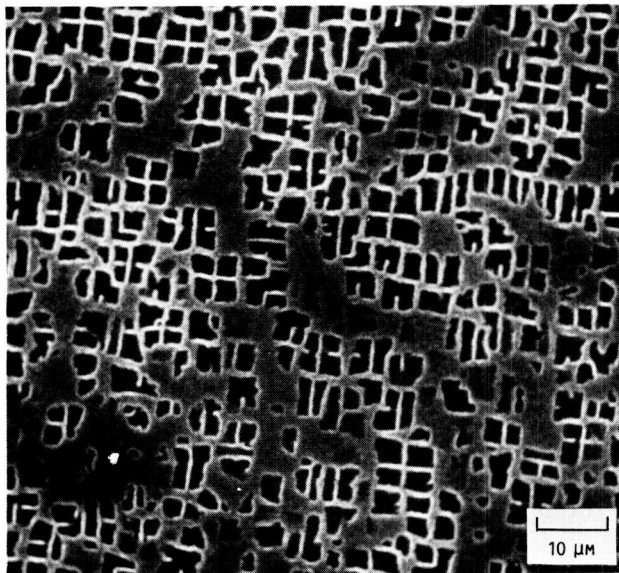
## REFERENCES

1. Bill, R.C., et al.: Preliminary Study of Thermomechanical Fatigue of Polycrystalline MAR-M 200. NASA TP-2280, AVSCOM-TR-83-C-6, 1984.
2. Halford, G.R.: Low Cycle Thermal Fatigue. NASA TM-87225, 1986.
3. Kaufman, M.: Examination of the Influence of Coatings on Thin Superalloy Sections: Volume 1: Description and Analysis. NASA CR-134791, 1974.
4. Halford, G.R., et al.: Bithermal Fatigue, a Link Between Isothermal and Thermomechanical Fatigue. Low Cycle Fatigue, ASTM STP-942, H.D. Solomon, et al., eds., American Society for Testing and Materials, 1988, pp. 625-637.
5. Miner, R.V., et al.: Orientation and Temperature Dependence of Some Mechanical Properties of the Single-Crystal Nickel-Base Superalloy René N4: Part I, Tensile Behavior. Metall. Trans. A, vol. 17, no. 3, Mar. 1986, pp. 491-496.
6. Gabb, T.P.; Gayda, J.; and Miner, R.V.: Orientation and Temperature Dependence of Some Mechanical Properties of the Single-Crystal Nickel-Base Superalloy René N4: Part II, Low Cycle Fatigue Behavior. Metall. Trans. A, vol. 17, no. 3, Mar. 1986, pp. 497-505.
7. Gayda, J., et al.: Bithermal Low-Cycle Fatigue Behavior of a NiCoCrAlY-Coated Single Crystal Superalloy. NASA TM-89831, 1987.
8. Schneider, K.; and Grunling, H.W.: Mechanical Aspects of High Temperature Coatings. Thin Solid Films, vol. 107, no. 4, 1983, pp. 395-416.
9. Strangman, T.E.; and Hopkins, S.W.: Thermal Fatigue of Coated Superalloys. Am. Ceram. Soc. Bul., vol. 55, no. 3, Mar. 1976, pp. 304-307.

TABLE I.- LCF DATA

| Specimen number | Test type         | Strainranges, at 1/2 life percentages |         |           | Cycles to failure |
|-----------------|-------------------|---------------------------------------|---------|-----------|-------------------|
|                 |                   | Total                                 | Elastic | Inelastic |                   |
| N20             | B760 <sup>a</sup> | 2.030                                 | 1.746   | 0.284     | 397               |
| N28             | ↓                 | 1.880                                 | 1.715   | 0.165     | 723               |
| N17             | ↓                 | 1.837                                 | 1.727   | 0.110     | 930               |
| N12             | ↓                 | 1.549                                 | 1.549   | 0.000     | 6739              |
| N7              | C760 <sup>b</sup> | 1.634                                 | 1.546   | 0.088     | 504               |
| N10             | C760              | 2.284                                 | 1.924   | 0.360     | 124               |
| N6              | B982 <sup>c</sup> | 1.550                                 | 1.116   | 0.434     | 228               |
| N11             | B982              | 0.914                                 | 0.805   | 0.109     | 2225              |
| N9              | B982              | 0.710                                 | 0.650   | 0.060     | 4094              |
| N15             | C982 <sup>d</sup> | 2.448                                 | 1.248   | 1.200     | 70                |
| N53             | B00P <sup>e</sup> | 0.590                                 | 0.584   | 0.006     | 9284              |
| N63             | ↓                 | 1.090                                 | 1.074   | 0.016     | 693               |
| N50             | ↓                 | 1.694                                 | 1.554   | 0.140     | 185               |
| N62             | ↓                 | 0.860                                 | 0.852   | 0.008     | 1357              |
| N66             | ↓                 | 1.306                                 | 1.282   | 0.024     | 536               |
| N67             | C00P <sup>f</sup> | 1.244                                 | 0.972   | 0.046     | 521               |
| N44             | ↓                 | 0.822                                 | 0.804   | 0.018     | 1827              |
| N38             | ↓                 | 1.442                                 | 1.404   | 0.038     | 24                |
| N32             | ↓                 | 1.486                                 | 1.406   | 0.080     | 21                |
| N25             | ↓                 | 1.350                                 | 1.320   | 0.030     | 50                |
| N19             | ↓                 | 0.670                                 | 0.664   | 0.006     | 4391              |
| N57             | BIP <sup>g</sup>  | 1.106                                 | 1.080   | 0.026     | 2897              |
| N58             | ↓                 | 1.630                                 | 1.520   | 0.110     | 120               |
| N60             | ↓                 | 1.284                                 | 1.230   | 0.054     | 293               |
| N56             | ↓                 | 1.232                                 | 1.206   | 0.026     | 1095              |
| N65             | ↓                 | 1.312                                 | 1.280   | 0.032     | 295               |
| N49             | CIP <sup>h</sup>  | 1.090                                 | 1.050   | 0.040     | 1775              |
| N59             | CIP               | 1.350                                 | 1.306   | 0.044     | 451               |
| N55             | CIP               | 1.476                                 | 1.380   | 0.096     | 122               |

<sup>a</sup>760 °C isothermal cycling, bare.<sup>b</sup>760 °C isothermal cycling, coated.<sup>c</sup>982 °C isothermal cycling, bare.<sup>d</sup>982 °C isothermal cycling, coated.<sup>e</sup>Out-of-phase bithermal cycling, bare.<sup>f</sup>Out-of-phase bithermal cycling, coated.<sup>g</sup>In-phase bithermal cycling, bare.<sup>h</sup>In-phase bithermal cycling, coated.



ORIENTATION, [001]

FIGURE 1. - HEAT TREATED MICROSTRUCTURE OF RENÉ N4.

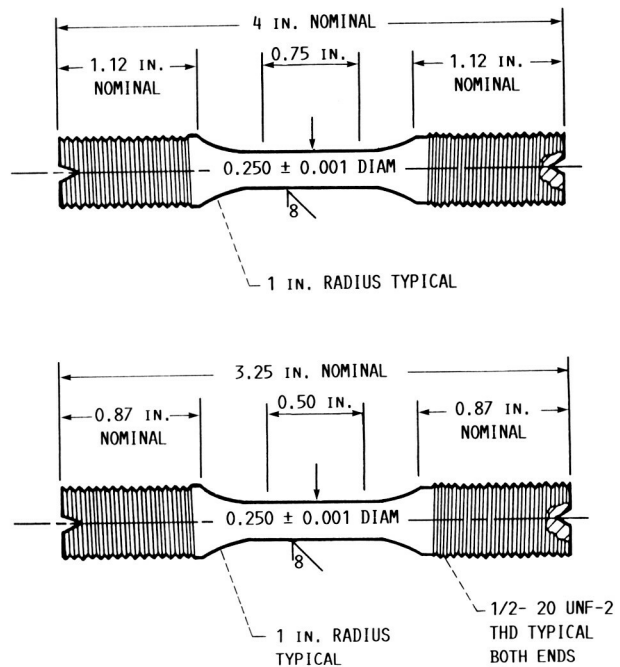


FIGURE 2. - LOW CYCLE FATIGUE SPECIMENS.

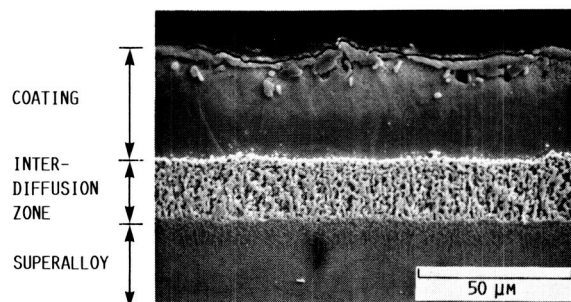
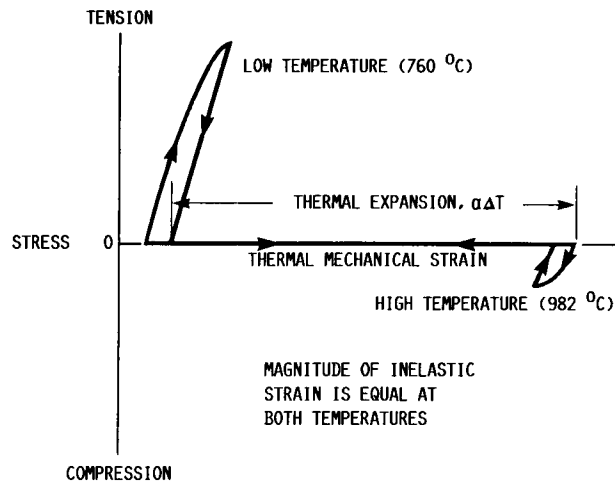
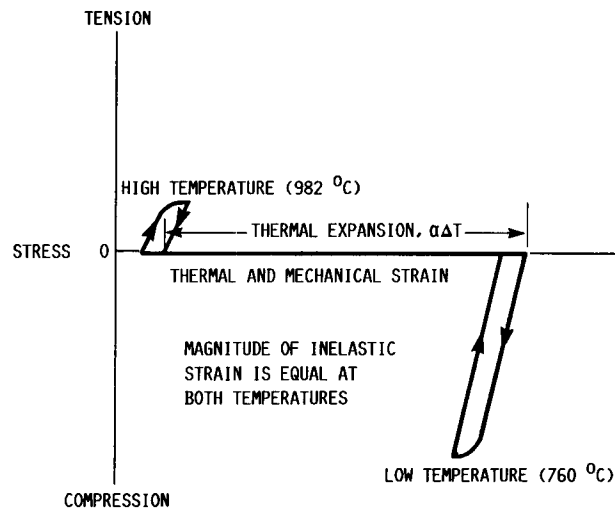


FIGURE 3. - MICROSTRUCTURE OF THE DIFFUSION ALUMINIDE COATING CODEP B-1.

ORIGINAL PAGE IS  
OF POOR QUALITY



(a) OUT-OF-PHASE.



(b) IN-PHASE.

FIGURE 4. - SCHEMATIC OF THE BITHERMAL FATIGUE CYCLE.

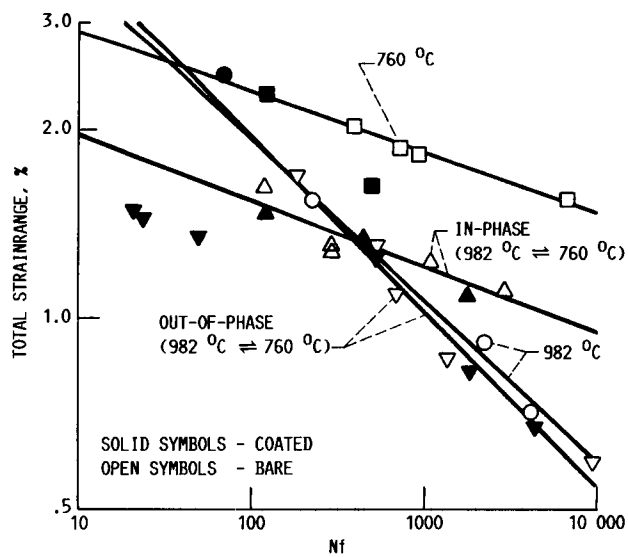


FIGURE 5. - COMPARISON OF FATIGUE LIVES ON A TOTAL STRAIN BASIS FOR BITHERMAL AND ISOTHERMAL CYCLING.

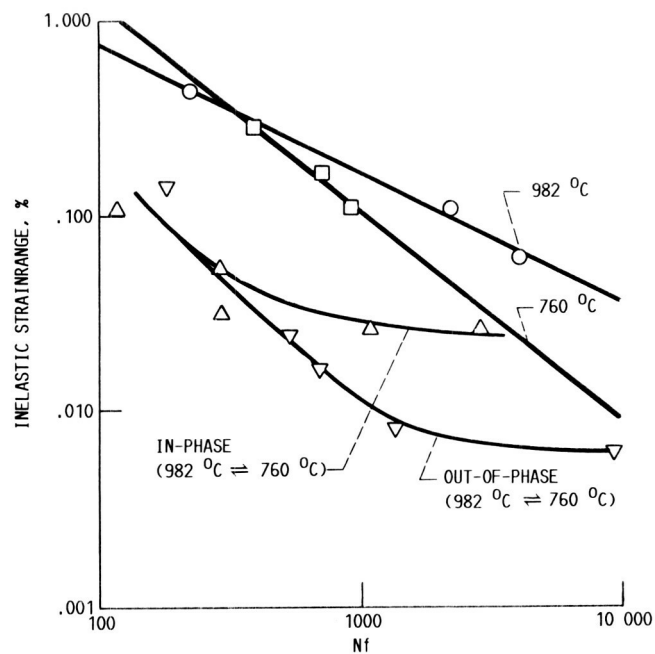
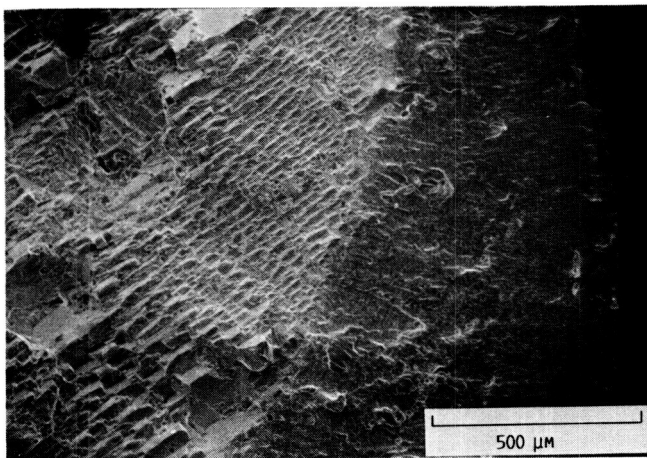
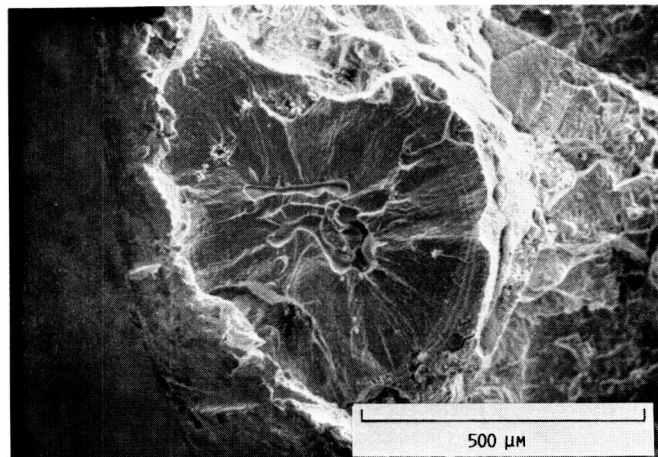


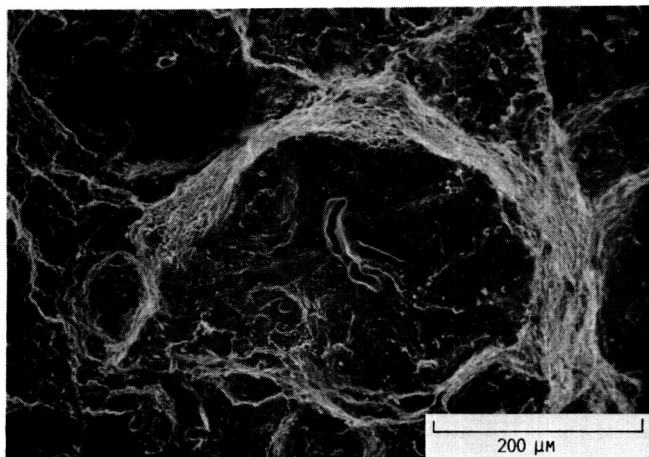
FIGURE 6. - COMPARISON OF FATIGUE LIVES ON AN INELASTIC STRAIN BASIS FOR BITHERMAL AND ISOTHERMAL CYCLING OF UNCOATED SPECIMENS.



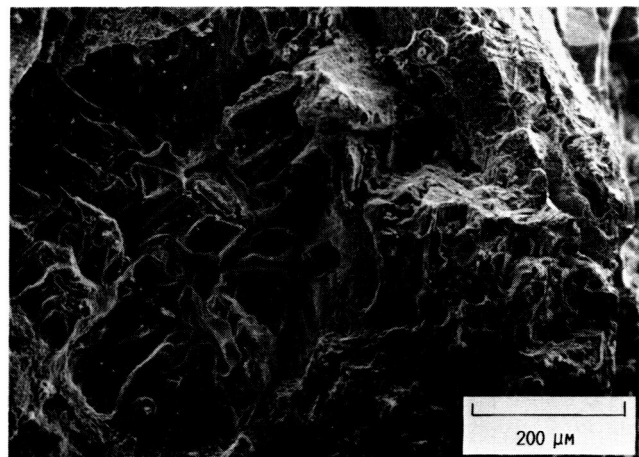
(a) 760 °C.



(a) BARE.



(b) 982 °C.

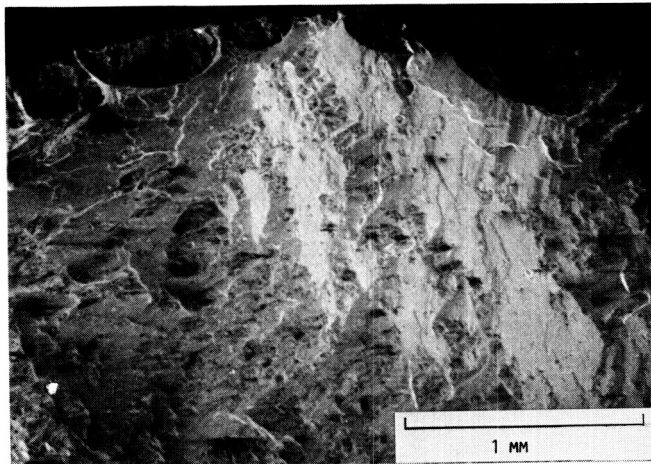


(b) COATED.

FIGURE 7. - FRACTURE SURFACE OF SPECIMENS ISOTHERMALLY FATIGUED.

FIGURE 8. - FRACTURE FEATURES FOR SPECIMENS CYCLED IN-PHASE.

ORIGINAL PAGE IS  
OF POOR QUALITY



(a) BARE.



(b) COATED.

FIGURE 9. - FRACTURE FEATURES FOR SPECIMENS CYCLED OUT-OF-PHASE.

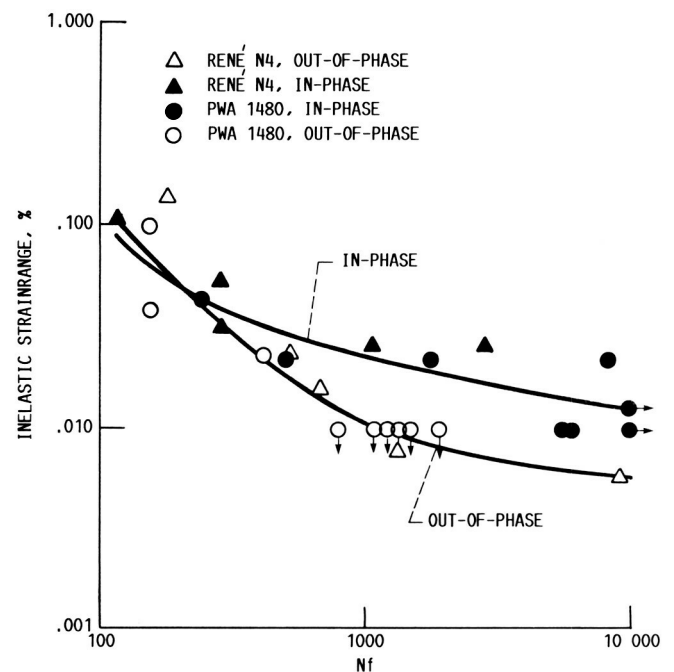


FIGURE 10. - PLOT OF FATIGUE LIFE AS A FUNCTION OF IN-ELASTIC STRAIN FOR BARE RENÉ N4 SPECIMENS AND FOR COATED AND BARE PWA 1480 FROM GAYDA ET AL. (7).

## Report Documentation Page

|   |  |  |   |   |  |
|---|--|--|---|---|--|
| 1. Report No.<br>NASA TM-100885   |  | 2. Government Accession No.                          |   | 3. Recipient's Catalog No.                                    |  |
| 4. Title and Subtitle<br><br>Bithermal Fatigue of a Nickel-Base Superalloy<br>Single Crystal  |  |  |   | 5. Report Date<br>May 1988                                    |  |
|   |  |  |   | 6. Performing Organization Code                               |  |
| 7. Author(s)<br>Michael J. Verrilli   |  |  |   | 8. Performing Organization Report No.<br>E-4118               |  |
|   |  |  |   | 10. Work Unit No.<br>553-13-00                                |  |
| 9. Performing Organization Name and Address<br>National Aeronautics and Space Administration<br>Lewis Research Center<br>Cleveland, Ohio 44135-3191   |  |  |   | 11. Contract or Grant No.                                     |  |
|   |  |  |   | 13. Type of Report and Period Covered<br>Technical Memorandum |  |
| 12. Sponsoring Agency Name and Address<br>National Aeronautics and Space Administration<br>Washington, D.C. 20546-0001  |  |  |   | 14. Sponsoring Agency Code                                    |  |
|   |  |  |   |   |  |
| 15. Supplementary Notes   |  |  |   |   |  |
| 16. Abstract<br><br>The thermomechanical fatigue behavior of a nickel-base superalloy single crystal was investigated using a bithermal test technique. The bithermal fatigue test was used as a simple alternative to the more complex thermomechanical fatigue test. Both in-phase and out-of-phase bithermal tests were performed on <001>-oriented coated and bare René N4 single crystals. In out-of-phase bithermal tests, the tensile and compressive halves of the cycle were applied isothermally at 760 and 982 °C respectively, while for the in-phase bithermal tests the temperature-loading sequence was reversed. The bithermal fatigue lives of bare specimens were shorter than the isothermal fatigue lives at either temperature extreme when compared on an inelastic strain basis. Both in-phase and out-of-phase bithermal fatigue life curves converged in the large strain regime and diverged in the small strain regime, out-of-phase resulting in the shortest lives. The coating had no effect on life for specimens cycled in-phase; however, the coating was detrimental for isothermal fatigue at 760 °C and for out-of-phase fatigue under large strains. |  |  |   |   |  |
| 17. Key Words (Suggested by Author(s))<br><br>Thermomechanical fatigue; Superalloys;<br>Aluminide coatings; Low cycle fatigue;<br>Oxidation; Crack initiation   |  |  | 18. Distribution Statement<br><br>Unclassified - Unlimited<br>Subject Category 26 |   |  |
| 19. Security Classif. (of this report)<br>Unclassified  |  | 20. Security Classif. (of this page)<br>Unclassified |   | 21. No of pages<br>14   |  |
|   |  |  |   | 22. Price*<br>A02   |  |